

# XRD, Raman and FT-IR spectroscopic observations of nanosized TiO<sub>2</sub> synthesized by the sol–gel method based on an esterification reaction

M. Ivanda<sup>a</sup>, S. Musić<sup>a</sup>, S. Popović<sup>b</sup>, M. Gotić<sup>a,\*</sup>

<sup>a</sup>Ruđer Bošković Institute, P.O. Box 1016, 10001 Zagreb, Croatia

<sup>b</sup>Faculty of Science, Department of Physics, University of Zagreb, P.O. Box 162, 10001 Zagreb, Croatia

Received 24 August 1998; accepted 19 October 1998

## Abstract

Ti(IV)-isopropoxide was hydrolyzed with water molecules generated “in situ” by an esterification between carboxylic acid and alcohol providing excellent control of the hydrolysis and condensation rate. Raman and FT-IR spectra of the TiO<sub>2</sub>–acetate precursor suggested that the organic ligand is chemically bound to the titanium. With heating of the TiO<sub>2</sub>–acetate precursor up to 320°C, the surface area increased from 3 to 280 m<sup>2</sup> g<sup>-1</sup>. The organic component completely decomposed above 320°C. With a further increase in temperature, the surface area of the nanocrystalline anatase gradually decreased. The method of low-frequency Raman scattering was used to determine the particle size in dependence on experimental conditions, and a good agreement was obtained with the crystallite size determination using the Scherrer method. © 1999 Elsevier Science B.V. All rights reserved.

**Keywords:** Sol–gel; TiO<sub>2</sub>; Nanocrystalline anatase; XRD; Raman; FT-IR; BET

## 1. Introduction

The photocatalytic activity of nanosized TiO<sub>2</sub> powder strongly depends on its microstructural and physical properties. For this reason, many researchers have extensively investigated the relation between the synthesis conditions and the properties of nanosized TiO<sub>2</sub> powder, such as surface area, total pore volume, particle and pore size distribution, crystallinity, thermal stability, phase composition etc. Nanosized TiO<sub>2</sub> powders are usually synthesized by sol–gel processing based on the hydrolysis and polycondensation reactions of Ti(IV)-alkoxide. However, the high

hydrolysis rate of Ti(IV)-alkoxide may cause uncontrolled local precipitation, producing optical and photocatalytic losses in the nanosized TiO<sub>2</sub> material. There are various approaches to control the hydrolysis and condensation rates and the relative rate of the hydrolysis/polycondensation reactions during the sol–gel processing, such as oligomerization, alcohol interchange, acid/base catalysis, ligand complexation (acac, oxalate, citrate), steric hindrance with large polymer molecules (HPC, PEG) etc. In the present work, excellent control of the hydrolysis rate of Ti(IV)-isopropoxide through an esterification reaction between carboxylic acid (acetic, formic, oxalic) and alcohol (ethanol, amyl) was achieved. The results of an investigation of nanosized TiO<sub>2</sub> particles obtained by an esterification reaction will be discussed.

\* Corresponding author.

E-mail address: gotic@rudjer.irb.hr (M. Gotić)

Table 1

Experimental conditions for the preparation of TiO<sub>2</sub> samples using sol–gel processing based on an esterification reaction

Sample	Volume of Ti(O <sup>i</sup> Pr) <sub>4</sub>	Volume of alcohol <sup>a</sup>	Volume of carboxylic acid <sup>b</sup>	Time and temperature of refluxing	Time and temperature of drying
AC1	25 ml	200 ml EtOH	80 ml H <sub>4</sub> C <sub>2</sub> O <sub>2</sub>	6 h at 100°C	88 h at 60°C
AC2	25 ml	50 ml EtOH	25 ml H <sub>4</sub> C <sub>2</sub> O <sub>2</sub>	8 h at 70°C	35 h at 60°C
AC3	25 ml	50 ml AmOH	25 ml H <sub>4</sub> C <sub>2</sub> O <sub>2</sub>	4 h at 100°C	90 h at 60°C
FOR1	25 ml	50 ml EtOH	25 ml H <sub>2</sub> CO <sub>2</sub>	4 h at 70°C	72 h at 60°C
FOR2	25 ml	50 ml AmOH	25 ml H <sub>2</sub> CO <sub>2</sub>	4 h at 90°C	90 h at 60°C
OX1	25 ml	75 ml EtOH	30.4 g H <sub>2</sub> C <sub>2</sub> O <sub>4</sub>	5 h at 70°C	90 h at 60°C

<sup>a</sup> Et = ethyl, Am = Amyl.<sup>b</sup> H<sub>4</sub>C<sub>2</sub>O<sub>2</sub> = acetic acid, H<sub>2</sub>CO<sub>2</sub> = formic acid, H<sub>2</sub>C<sub>2</sub>O<sub>4</sub> = oxalic acid.

## 2. Experimental

Ti(IV)-isopropoxide supplied by Aldrich was used. Special attention was paid in removing the water and purification of the chemicals. A small quantity of absolute ethanol (Kemika, Zagreb) in the presence of extra pure magnesium powder and iodine as a catalyst, was heated until all the magnesium was converted to magnesium ethoxide. One liter of absolute ethanol was added. After 3 h of refluxing, the absolute alcohol was distilled off. Absolute amyl alcohol supplied by Merck was refluxed 6 h before using. Traces of water from glacial acetic acid supplied by Kemika were removed by adding some acetic anhydride in the presence of a small quantity of CrO<sub>3</sub>, refluxed for several hours and then fractionally

distilled off. Formic acid was dried by refluxing it with freshly prepared anhydrous CuSO<sub>4</sub> for several days and distilling it under vacuum. In order to obtain anhydrous oxalic acid, H<sub>2</sub>C<sub>2</sub>O<sub>4</sub>·2H<sub>2</sub>O supplied by Merck was recrystallized and dried at 115°C for at least 24 h.

Experiments were performed in an oil bath using a specially designed glass apparatus to prevent contact between the precipitation system and moisture in air. Before bubbling N<sub>2</sub> gas into the reaction vessel, extra pure nitrogen (> 99.999% N<sub>2</sub>) was additionally purified through a pyrogallol and conc. H<sub>2</sub>SO<sub>4</sub> bubblers (traps) and then through two tubes with silica gel. Ti(IV)-isopropoxide was homogeneously hydrolyzed through an esterification reaction between carboxylic acid and alcohol, R'COOH + ROH → R'COOR +

Table 2

XRD phase analysis, crystallite size (Scherrer method) and surface area (BET) of selected samples

Sample	Temperature of heating (°C)	XRD phase composition	Crystallite size (nm)	Surface area (m <sup>2</sup> g <sup>-1</sup> )
FOR1	as prepared	Anatase <sup>a</sup> + amorphous phase	6 ± 1	346.7
AC1	as prepared	<sup>b</sup> Amorphous		3.2
AC1a	170	Amorphous		69.5
AC1b	270	Amorphous		—
AC1c	320	Amorphous		280.6
AC1d	370	Anatase <sup>c</sup> + amorphous phase	9 ± 1	111.8
AC1e	425	Anatase <sup>d</sup> + amorphous phase	12 ± 1	77.3
AC1f	480	Anatase <sup>e</sup> + amorphous phase	17 ± 1	46.6
AC2	as prepared	<sup>b</sup> Amorphous		3.1

<sup>a</sup> Very broadened diffraction lines.<sup>b</sup> Extremely broadened diffraction line at the position of the anatase line at  $\theta = 12.5^\circ$ .<sup>c</sup> Broadened diffraction lines.<sup>d</sup> Broadened diffraction lines but lesser than that in AC1d.<sup>e</sup> Broadened diffraction lines but lesser than that in AC1e.

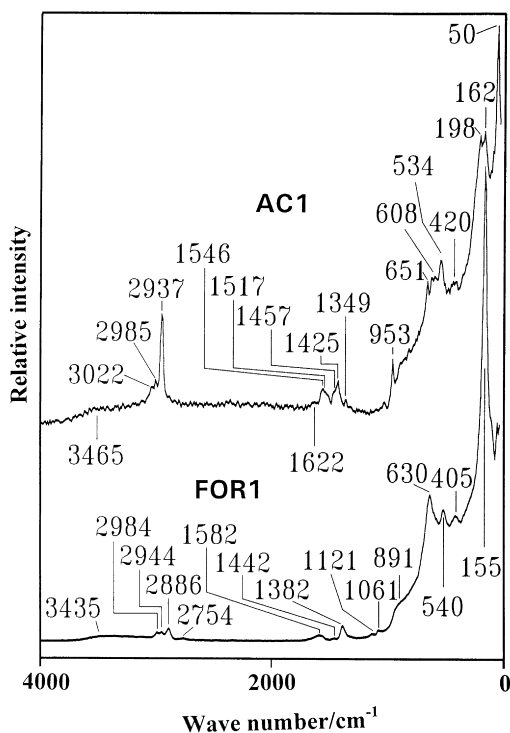


Fig. 1. Raman spectra of samples AC1 and FOR1 synthesized in the presence of acetic acid and in the presence of formic acid, respectively.

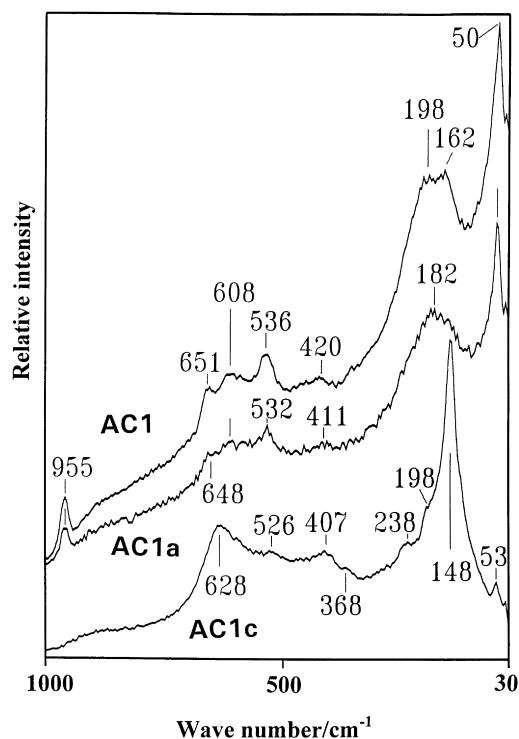


Fig. 2. Raman spectra in the wave number range of  $1000$  to  $30\text{ cm}^{-1}$  of sample AC1 and its thermal decomposition products at  $170^\circ\text{C}$  and  $320^\circ\text{C}$ , samples AC1a and AC1c, respectively.

$\text{H}_2\text{O}$ . The suspension was refluxed ( $70^\circ\text{C}$  to  $110^\circ\text{C}$ ) and stirred constantly at 500 to 1000 r.p.m. The experimental conditions for the preparation of organically modified  $\text{TiO}_2$  samples are given in Table 1. The  $\text{TiO}_2$  suspensions were dried in Petri dishes at  $60^\circ\text{C}$ . The products were analyzed as synthesized or thermally treated in a tubular furnace with a temperature stability of  $\pm 2^\circ\text{C}$ . Samples were characterized by XRD, Raman and FT-IR spectroscopies, and BET.

### 3. Results and discussion

The results of XRD analysis are summarized in Table 2. Sample AC1 can be assigned to an amorphous-like  $\text{TiO}_2$ -acetate phase and an extremely broadened diffraction line at the position of the anatase line at  $\theta = 12.5^\circ$  was observed. After heating sample AC1 at  $170^\circ\text{C}$ , extremely broad diffraction maximum completely disappeared. With

the additional heating of sample AC1 at  $370^\circ\text{C}$ ,  $425^\circ\text{C}$  and  $480^\circ\text{C}$ , XRD patterns corresponding to the anatase phase, appeared. The average crystallite size estimated from the broadening of the diffraction line increased from 9 to 17 nm with an increase of the temperature up to  $480^\circ\text{C}$ . Sample FOR1, synthesized in the presence of formic acid, corresponded to anatase phase with a very broad crystallite size distribution having maximum at 6 nm.

The Raman spectrum of sample AC1 (Fig. 1) exhibited a sharp and strong band at  $2937\text{ cm}^{-1}$  associated with the bands at  $3022$  and  $2985\text{ cm}^{-1}$ , as a result of the stretching vibrations of  $\text{CH}_2$  and  $\text{CH}_3$  groups of unhydrolyzed alkoxide. The same bands are also present in the FT-IR spectrum, but they are less visible vibrations because of the screened effect of the KBr matrix. The very broad band at  $420$  to  $407$  and the broad band at  $608$  to  $628\text{ cm}^{-1}$  in Raman spectra (Fig. 2) are related to short range order of the octahedrally coordinated titanium and their presence in Raman

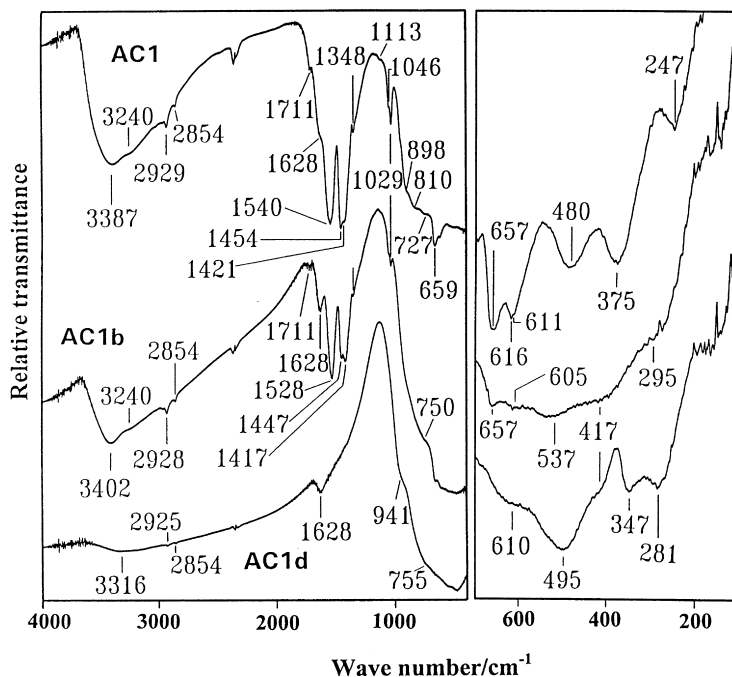


Fig. 3. Infrared spectra of the sample AC1 and its thermal decomposition products at 270 and 370°C (samples AC1b and AC1d, respectively), collected in the wave number range of 4000 to 400 cm<sup>-1</sup> in a KBr pellet (mid-infrared region) and in the wave number range of 700 to 150 cm<sup>-1</sup> (far-infrared region) in a polyethylene foil.

spectrum, without the band at 144 cm<sup>-1</sup> suggested that there is no long range ordered structure of crystalline anatase or rutile phase. The IR bands at 3387 and 3236 cm<sup>-1</sup> (Fig. 3) showed the presence of -OH stretching vibrations in sample AC1, while the shoulder at 1628 cm<sup>-1</sup> can be ascribed to the bending vibrations of adsorbed H<sub>2</sub>O molecules. The band at 1628 cm<sup>-1</sup> is strongly screened by the dominant bands at 1540 and 1454 cm<sup>-1</sup>, which corresponds to the symmetric and asymmetric vibrations of C(=O)O<sup>-</sup>, and can be ascribed to the presence of CH<sub>3</sub>C(=O)O<sup>-</sup> bidentate chelating or a bridging group covalently bound to titanium [1]. Thermal treatment of sample AC1 caused the acetate groups to decompose, as visible from the decrease of the relative intensity of the bands at 1540 and 1454 cm<sup>-1</sup> in the FT-IR spectra and the corresponding bands in the Raman spectra. These bands disappeared after thermal treatment at 350°C.

Generally in Raman spectra, the most intensive band at 144 cm<sup>-1</sup> is associated with the anatase crystalline phase. For sample FOR1, this band is

positioned at 155 cm<sup>-1</sup>. Sample AC1 showed the band at 162 cm<sup>-1</sup> associated with the band at 198 cm<sup>-1</sup> (Fig. 1), and they could be ascribed to an amorphous phase.

The authors of the present work [2] applied the low-frequency Raman method for the first time to the particle size determination of “pure” nanosized oxide particles (TiO<sub>2</sub>) which were not inside any matrix. Recently, the same method was applied to the size determination of nanosized SnO<sub>2</sub> particles [3]. The low frequency Raman spectra of samples AC1, AC1c, AC1d and AC1e (denoted as **a**, **b**, **c**, and **d**, respectively) are shown in Fig. 4. The amorphous like TiO<sub>2</sub>-acetate precursor (sample AC1, denoted as **a**) shows 2 low-frequency Raman peaks at 60 and 22 cm<sup>-1</sup>. The maximum at 22 cm<sup>-1</sup> corresponds to TiO<sub>2</sub> particles of 9 nm, while the maximum at 60 cm<sup>-1</sup> could be associated with particles containing an organic component. After the thermal treatment of Sample AC1 above 360°C, acetate decomposed completely and consequently, the maximum at 60 cm<sup>-1</sup> disappeared. A shift of the

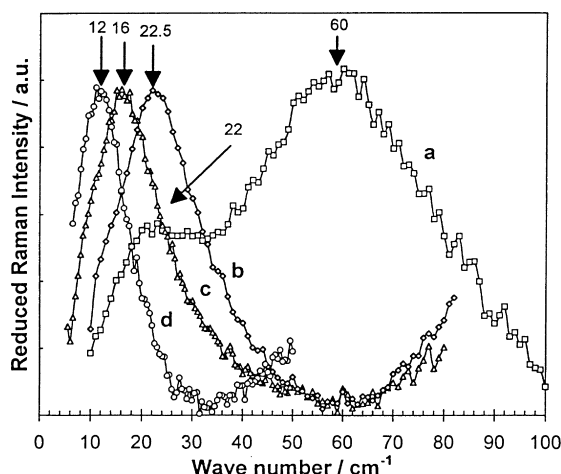


Fig. 4. The low frequency Raman spectra of samples AC1, AC1c, AC1d and AC1e (denoted as **a**, **b**, **c** and **d**, respectively) in the wave number range of up to  $100\text{ cm}^{-1}$ . The numbers under the arrows show the positions of the low-frequency maxima. The maximum at  $22\text{ cm}^{-1}$  corresponds to  $\text{TiO}_2$  particles of  $9\text{ nm}$ , while the maximum at  $60\text{ cm}^{-1}$  could be associated with particles containing an organic component. The shift of the maximum at  $22.5$  to  $12\text{ cm}^{-1}$  corresponds to the increase of anatase particle size from  $10$  to  $18\text{ nm}$ , which is in a good agreement with crystallite size values obtained by XRD ( $9$  to  $17\text{ nm}$ ).

maximum from  $22.5$  to  $12\text{ cm}^{-1}$  with increasing temperature up to  $480^\circ\text{C}$  corresponded to the increasing of the anatase particle sizes from  $10$  to  $18\text{ nm}$ , which was in good agreement with the crystallite size values obtained by XRD ( $9$  to  $17\text{ nm}$ ).

Sample AC1 synthesized in the presence of acetic acid possessed a BET surface area of only  $3\text{ m}^2\text{ g}^{-1}$ .

After thermal treatment of up to  $320^\circ\text{C}$ , the surface area increased gradually to the value of  $280.6\text{ m}^2\text{ g}^{-1}$  (Table 2). This maximum BET surface corresponded to the minimum organic component present in the sample. Above  $320^\circ\text{C}$ , the organic component decomposed completely and nanocrystalline anatase was formed as a single phase. The surface area by the BET of formed nanocrystalline anatase decreased from  $112$  to  $47\text{ m}^2\text{ g}^{-1}$  as temperature increased from  $370^\circ\text{C}$  to  $480^\circ\text{C}$ , which was in accordance with an increase in anatase particle size from  $10$  to  $18\text{ nm}$ , as determined by low-frequency Raman scattering [4,5].

## Acknowledgement

Authors wish to thank Mr. Strečko Karašić for performing BET measurements.

## References

- [1] I. Laaziz, A. Larbot, A. Julbe, C. Guizard, L. Cot, J. Solid State Chem. 98 (1992) 393.
- [2] M. Gotić, M. Ivanda, A. Sekulić, S. Musić, S. Popović, A. Turković, K. Furić, Mater. Lett. 28 (1996) 225.
- [3] A. Dieguez, A. Romano-Rodriguez, J.R. Morante, N. Barsan, U. Weimar, W. Gopel, Appl. Phys. Lett. 71 (1997) 1957.
- [4] S. Musić, M. Gotić, M. Ivanda, S. Popović, A. Turković, R. Trojko, A. Sekulić, K. Furić, Mater. Sci. Engng B47 (1997) 33.
- [5] M. Ivanda, S. Musić, M. Gotić, A. Turković, A.M. Tonejc, O. Gamulin, J. Mol. Struct. 480-481 (1999) 641–644.